EF24, a novel synthetic curcumin analog, induces apoptosis in cancer cells via a redox-dependent mechanism

Brian K. Adams[a–c], Jiyang Cai[d,e], Jeff Armstrong[b], Marike Herold[c], Yang J. Lu[b,c], Aiming Sun[c], James P. Snyder[c], Dennis C. Liotta[c], Dean P. Jones[d] and Mamoru Shoji[b,d]

In this study, we show that the novel synthetic curcumin analog, EF24, induces cell cycle arrest and apoptosis by means of a redox-dependent mechanism in MDA-MB-231 human breast cancer cells and DU-145 human prostate cancer cells. Cell cycle analysis demonstrated that EF24 causes a G_2/M arrest in both cell lines, and that this cell cycle arrest is followed by the induction of apoptosis as evidenced by caspase-3 activation, phosphatidylserine externalization and an increased number of cells with a sub-G_1 DNA fraction. In addition, we demonstrate that EF24 induces a depolarization of the mitochondrial membrane potential, suggesting that the compound may also induce apoptosis by altering mitochondrial function. EF24, like curcumin, serves as a Michael acceptor reacting with glutathione (GSH) and thioredoxin 1. Reaction of EF24 with these agents *in vivo* significantly reduced intracellular GSH as well as oxidized GSH in both the wild-type and Bcl-x_L overexpressing HT29 human colon cancer cells. We therefore propose that the anticancer effect of a novel curcumin analog, EF24, is mediated in part by redox-mediated induction of apoptosis. *Anti-Cancer Drugs* 16:263–275 © 2005 Lippincott Williams & Wilkins.

Anti-Cancer Drugs 2005, **16**:263–275

Keywords: apoptosis, caspase, DNA fragmentation, EF24, G_2/M cell cycle arrest, glutathione, mitochondrial membrane depolarization, oxidized glutathione, phosphatidylserine externalization, reactive oxygen species, reduction–oxidation (redox), synthetic curcumin analog

[a]Program in Molecular and Systems Pharmacology, [b]Winship Cancer Institute, [c]Department of Chemistry and [d]Department of Medicine, Emory University, Atlanta, GA, USA and [e]Department of Ophthalmology and Visual Sciences, Vanderbilt University, Nashville, TN, USA.

Sponsorship: NIH grant CA82995 (M. S., D. C. L. and J. P. S.) and contract N01-CM-5600 (D. C. L. and J. P. S.), US Department of Defense, the Division of US Army DAMD17-00-1-0241 (M. S., D. C. L. and J. P. S.), a contract with the George Washington University Medical Center (M. S.), NIH grant ES 09047 (D. P. J.) and American Association for Cancer Research (J. C.).

J. C. and J. A. contributed equally to this work.

Correspondence to M. Shoji, Winship Cancer Institute, Emory University, Clinic B, Suite B4100, 1365-B Clifton Road, Atlanta, GA 30322, USA.
Tel: +1 404 727-3457; fax: +1 404 778-3965;
e-mail: mamoru_shoji@emoryhealthcare.org

Received 21 June 2004 **Revised form accepted** 10 November 2004

Introduction

Curcumin (diferuloylmethane) (Fig. 1), a major component of turmeric, is used as a coloring and flavoring agent in many food items, including curries and mustards. Although curcumin has traditionally been used in Indian folk medicine for a number of ailments, recent preclinical and clinical studies demonstrate that this phytochemical has a number of anticancer properties [1]. The pharmacological safety of curcumin has been demonstrated by its consumption for centuries at levels of up to 100 mg/day by people in certain countries [2]. One potential problem with the clinical use of curcumin is its low potency and poor absorption characteristics [3]; however, curcumin remains an ideal lead compound for the design of more effective analogs.

We recently synthesized approximately 100 curcumin analogs, and tested them for their anticancer and anti-angiogenesis properties. All of the novel compounds were more active than curcumin. One compound in particular, EF24 (Fig. 1), is more active and considerably less toxic than the commonly used chemotherapeutic drug cisplatin in anticancer screens [4]. EF24 was also effective in reducing the size of human breast tumors grown in nude mice [4].

Apoptosis is characterized by numerous biochemical and morphological changes in the cell including caspase activation (particularly caspase-3), phosphatidylserine (PS) exposure, cytoplasmic shrinkage and DNA fragmentation. Studies suggest that both oxidative stress and loss of mitochondrial membrane potential are causal events of apoptosis [5,6]. Anticancer agents that induce apoptosis at doses below those that display cytotoxicity to normal cells could be clinically useful. There is accumulating evidence that the efficiency of chemotherapeutic agents such as cisplatin, camptothecin and etoposide is related to the intrinsic propensity of the target tumor cells to respond to these agents by apoptosis [7].

In the present study, we have investigated the possible mechanisms by which the potent curcumin analog, EF24,

0959-4973

Fig. 1

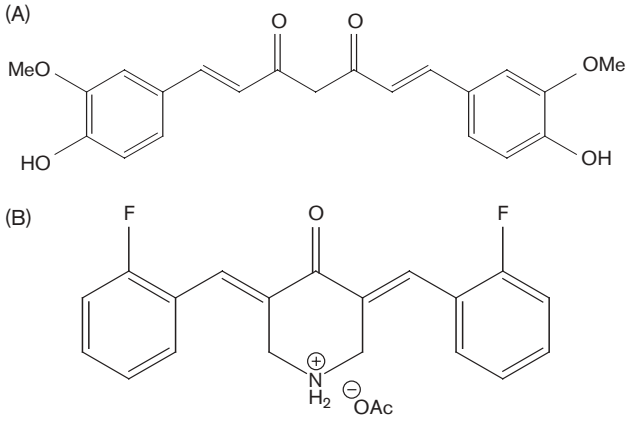

Chemical structures. The topological structures of curcumin (A) and EF24 (B).

exerts its anticancer effects. The results indicate that EF24 effectively penetrates and induces apoptosis in cultured human breast and prostate cancer cells. A rapid depletion of intracellular glutathione (GSH) was observed and that was not inhibited by overexpression of Bcl-x_L. The unique chemical properties and biological effects of EF24 suggest it represents a novel class of compounds that exert their anticancer activities by redox-dependent mechanisms.

Materials and methods

Cell culture

Human MDA-MB-231 breast cancer cells, DU-145 prostate cancer cells and HT29 colon cancer cells were purchased from ATCC (Rockville, MD). MEM-α medium, RPMI 1640 medium, McCoy's medium, penicillin, streptomycin and L-glutamine were purchased from Gibco/BRL (Rockville, MD) and Mediatech (Herndon, VA). Fetal bovine serum (FBS) was purchased from Atlanta Biologicals (Atlanta, GA). The MDA-MB-231 cells, and the DU-145 and the HT29 cells (wild-type and overexpressed Bcl-x_L) were maintained in MEM-α medium, RPMI 7951 and McCoy's medium, respectively, containing 10% FBS, penicillin (100 U/ml), streptomycin (100 μg/ml) and 2 mM L-glutamine. Overexpression of Bcl-x_L in HT29 cells is described elsewhere [8]. Cells were incubated at 37°C in 5% CO_2/95% air in a humid atmosphere. In order to avoid mutational changes of cell lines, cells were expanded in culture, aliquotted and stored in a liquid nitrogen freezer when purchased from the ATCC. Cells subjected to less than 20 passages were used.

5-Bromo-2′-deoxyuridine (BrdU) cell proliferation assay

This assay was performed as previously described with modifications [9]. DU-145 and MDA-MB-231 cells were plated at a density of 20 000 cells/well on 96-well plates and incubated overnight allowing cells to adhere. Following treatment with EF24 or dimethylsulfoxide (DMSO) for various periods of time, BrdU incorporation into proliferating cells was measured according to the directions supplied by Calbiochem (San Diego, CA) in their BrdU Cell Proliferation Assay Kit. During the final 18 h of culture, the BrdU label was added to the wells of the microplate, thereby incorporating it into the DNA of dividing cells. The cells were then fixed, permeabilized and the DNA denatured. Detector anti-BrdU monoclonal antibody, which binds to incorporated BrdU, was pipetted into the wells and allowed to incubate for 1 h at room temperature. Unbound antibody was washed away with a solution of phosphate-buffered saline (PBS) and surfactant. Then, horseradish peroxidase (HRP)-conjugated goat anti-mouse antibody, which binds to the detector antibody, was added for 30 min at room temperature. HRP catalyzes the conversion of the chromagenic substrate tetramethylbenzidine (TMB) from a colorless solution to a blue solution, the intensity of which is proportional to the amount of incorporated BrdU in the cells. The wells were then washed 3 times and flooded with deionized water. TMB was then added to the wells for 15 min at room temperature in the dark. The reaction was stopped using sulfuric acid and the colored reaction product was quantified at a wavelength of 450 nm using a Bio-Tek (Winooski, VT) microplate reader.

Cell cycle analysis

This assay was performed as previously described [10]. DU-145 and MDA-MB-231 cells were plated at a density of 1×10^6 cells/well on six-well plates. After treatment with EF24 or DMSO for various periods of time, both detached and attached cells were collected into flow cytometry tubes and centrifuged at 1000 r.p.m. for 5 min to obtain a cell pellet. The supernatant was discarded, and the cells were washed with PBS and re-centrifuged. The supernatant was discarded again and the cells were suspended in a solution of PBS/5 mM EDTA. An equal volume of ethanol was added to the cells and the tubes were incubated for 30 min at room temperature. The tubes were then centrifuged, the supernatant discarded and the cells resuspended in PBS/5 mM EDTA. RNase A (Sigma, St Louis, MO) was then added (40 μg/ml final concentration) and the tubes allowed to incubate for 30 min at room temperature. Propidium iodide (PI; Roche, Indianapolis, IN) was added to the tubes at a final concentration of 0.05 mg/ml and the cell cycle analysis was performed with a Becton Dickinson (Mountain View, CA) FACScan using an FL2 detector having a bandpass filter with specifications 585 ± 21 nm. In each analysis, 10 000 events were recorded.

Measurement of mitochondrial membrane potential

Measurement of the mitochondrial membrane potential was performed using the dye 5,5′,6,6′-tetrachloro-1,

1′,3,3′-tetraethylbenzimidazolylcarbocyanine iodide (JC-1) as previously described with slight modifications [11,12]. JC-1 (Sigma-Aldrich) is a cationic dye that exhibits potential dependent accumulation in the mitochondria as indicated by a fluorescent shift from green (around 525 nm) to red (around 590 nm). JC-1 emits a red color when sequestered in the mitochondria of healthy cells, but emits a green color when it is localized in the cytoplasm. Cells undergoing apoptosis are no longer able to retain the dye in the mitochondria. Consequently, they are detected as green-colored cells by flow cytometry. Consequently, mitochondrial depolarization is indicated by a decrease in the red/green fluorescence ratio. DU-145 and MDA-MB-231 cells were plated at a density of 1×10^6 cells/well on six-well plates. After treatment with EF24 or DMSO for various periods of time, both detached and attached cells were collected into flow cytometry tubes, and centrifuged at 1000 r.p.m. for 5 min to obtain a cell pellet. After resuspension in a solution of PBS containing 10 mM glucose, the cells were incubated with JC-1 (1 μg/ml) for 30 min at 37°C and washed with PBS. JC-1 fluorescence was measured immediately with a Becton Dickinson FACScan using both an FL1 detector (green fluorescence) having a bandpass filter with specifications 530 ± 15 nm and an FL2 detector (red fluorescence) having a bandpass filter with specifications 585 ± 21 nm. In each analysis, 10 000 events were recorded.

Caspase-3 activation

This assay was performed as previously described [13]. DU-145 and MDA-MB-231 cells were plated at a density of 1×10^6 cells/well on six-well plates. After treatment with the compound or DMSO for various periods of time, both detached and attached cells were collected into flow cytometry tubes and centrifuged at 1000 r.p.m. for 5 min to obtain a cell pellet. The supernatant was discarded and the cells were processed according to the directions in the Caspase-3 Intracellular Activity Assay Kit II (PhiPhiLux G_2D_2) from Calbiochem (San Diego, CA). Then, 50 μl of PhiPhiLux G_2D_2 substrate solution in RPMI 1640 medium was added to the cell pellets and incubated in a 5% CO_2 incubator at 37°C for 1 h. PhiPhiLux is a peptide substrate for caspase-3 that has been conjugated to two fluorophores (G_2D_2). The substrate contains the sequence GDEVDGI, with the caspase cleavage site underlined. When the folded peptide is cleaved, the fluorophores provide a high intensity fluorescent signal with the following peak characteristics; $\lambda_{ex} = 552$ nm and $\lambda_{em} = 580$ nm. Following incubation, the cells were washed with an ice-cold dilution buffer (supplied by Calbiochem). Flow cytometric analysis was performed with a Becton Dickinson FACScan using an FL2 detector having a bandpass filter with specifications 585 ± 21 nm (the FL2 channel with excitation at 488 nm). In each analysis, 10 000 events were recorded.

Annexin-V staining

Double staining for Annexin-V–fluorescein isothiocyanate (FITC) binding and for cellular DNA using PI was performed as previously described [14]. Annexin-V is a phospholipid binding protein with an extremely high affinity for PS. DU-145 and MDA-MB-231 cells were plated at a density of 1×10^6 cells/well on six-well plates. After treatment with the compound or DMSO for various periods of time, both detached and attached cells were collected into flow cytometry tubes and centrifuged at 1000 r.p.m. for 5 min to obtain a cell pellet. After the supernatant was discarded, the cells were washed twice with cold PBS and resuspended in 1 ml binding buffer (BD PharMingen, San Diego, CA). The cells were then stained with Annexin-V–FITC and PI according to the protocol described by BD PharMingen. Briefly, 5 μl of Annexin-V–FITC and 10 μl of PI were added to a 100 μl solution of cells and the solution was incubated for 15 min at room temperature in the dark. Binding buffer was then added, and early and late apoptosis was visualized by constructing a dot-plot using a Becton Dickinson FACScan. Green fluorescence from the Annexin-V–FITC was measured using an FL1 detector having a bandpass filter with specifications 530 ± 15 nm. Red fluorescence from PI was measured using an FL2 detector having a bandpass filter with specifications 585 ± 21 nm. In each analysis, 10 000 events were recorded.

Measurement of reactive oxygen species (ROS)

Measurement of intracellular ROS was performed using the peroxide-sensitive fluorescent probe 2′,7′-dichlorofluorescein diacetate (DCF-DA) (Sigma) as previously described with slight modifications [10]. DU-145 and MDA-MB-231 cells were plated at a density of 1×10^6 cells/well on six-well plates. After treatment with EF24 or DMSO for various periods of time, both detached and attached cells were collected into flow cytometry tubes, and centrifuged at 1000 r.p.m. for 5 min to obtain a cell pellet. After resuspension in a solution of PBS containing 10 mM glucose, the cells were incubated with DCF-DA (50 μM) for 15 min at 37°C in the dark. DCF fluorescence (an indicator of intracellular ROS production) was measured immediately with a Becton Dickinson FACScan using an FL1 detector having a bandpass filter with specifications 530 ± 15 nm. In each analysis, 10 000 events were recorded.

Measurement of interactions between EF24, GSH and thioredoxin-1 (Trx-1)

EF24 in PBS has an absorbance peak around 325 nm. To determine *in vitro* interactions, 20 μM EF24 was used to react with GSH and Trx-1 in 1 ml of PBS (pH 7.0) solution. The absorbance changes of the reactions were monitored at 325 nm for 10 min at 30°C. A decrease in absorbance indicated EF24 had reacted with GSH/Trx-1 and changed its spectroscopic character.

Determination of the effects of EF24 on intracellular GSH

HT29 human colon adenocarcinoma cells were treated with EF24 at 20 μM concentration for 90 min. HT29 cells with increased Bcl-x_L expression have been described elsewhere [8]. The cells were then extracted with 10% perchloric acid/0.2 M boric acid. Samples were derivatized with iodoacetic acid and dansyl chloride. The acid soluble GSH and oxidized GSH (GSSG) were then measured on a Waters 2690 Alliance HPLC system as described [15].

Results

Inhibition of cancer cell proliferation

BrdU incorporation

EF24 effectively inhibits the active synthesis of DNA in both DU-145 prostate cancer cells and MDA-MB-231 breast cancer cells (Fig. 2). Both cell lines were treated with various concentrations of the compound for 6, 12, 24, 48 and 72 h. At a drug concentration of 10 μM (10^{-5} M), BrdU incorporation is inhibited to 35% of control in the prostate cancer cell line after a 24 h treatment and is completely inhibited after treatment for 72 h. The compound demonstrates approximately 40% inhibition at 1 μM (10^{-6} M) after a 72-h treatment. In the breast cancer cells, EF24 induces complete growth arrest at 10 μM after only a 12-h treatment. Again, the compound demonstrates approximately 40% inhibition at 1 μM after treatment for 72 h.

Fig. 2

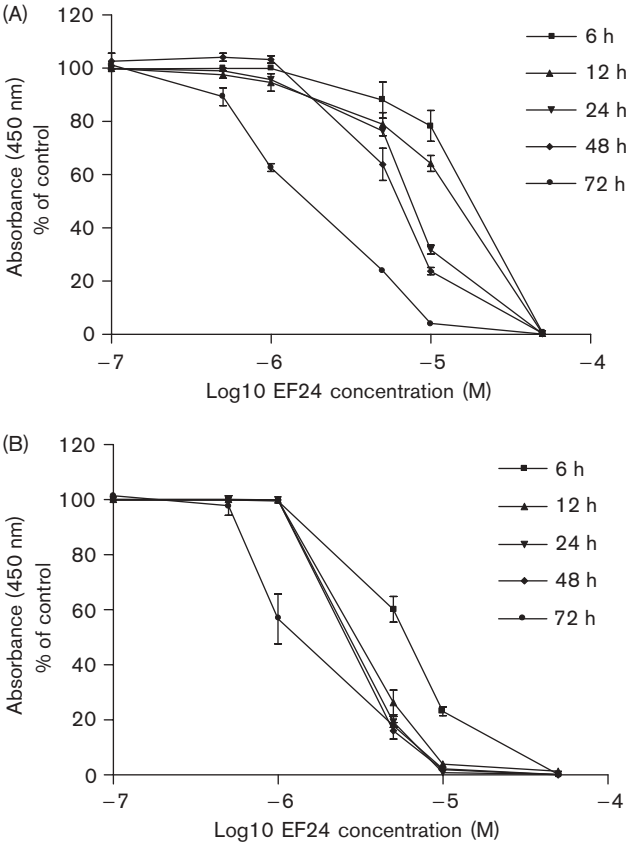

Inhibition of cancer cell proliferation by EF-24. DU-145 prostate cancer cells (A) and MDA-MB-231 breast cancer cells (B) were plated at 2×10^5 cells/well overnight, allowed to adhere, and treated with different concentrations of EF24 for 6, 12, 24, 48 and 72 h. The cells were then labeled with BrdU for 18 h and assayed as described in Materials and methods. The thymidine analog is incorporated into newly synthesized DNA strands of actively proliferating cells. Immunochemical detection of BrdU allows the assessment of the population of cells that are actively synthesizing DNA. Data points represent means ± SEM ($n = 3$).

Growth arrest in G_2/M, followed by sub-G_0/G_1 DNA accumulation

Flow cytometric analysis of the cell cycle was performed to determine the time course for the induction of DNA fragmentation by EF24, which is the final stage of apoptosis, and characterized by nuclear condensation and oligonucleosomal DNA fragmentation. Cells were treated with 20 μM EF24 for various times and histograms were constructed showing the percentage of cells in different phases of the cell cycle (G_1, S and G_2/M) as well as the percentage of cells with hypodiploid/fragmented DNA (sub-G_1/G_0). It is evident from the data in Fig. 3 that EF24 induces growth arrest in the G_2/M phase of the cell cycle. In the DU-145 cell line, the percentage of cells in G_2/M (M4 peak) after a 48-h treatment with EF24 (27.6%) was over 3-fold higher than the percentage of vehicle-treated cells in G_2/M (8.3%). In the EF24-treated MDA-MB-231 cell line, the percentage of cells in G_2/M was also higher (25.9%) than in control cells (16.1%) after 48 h. However, the G_2/M arrest in these cells was not as robust as that of the DU-145 cells. The percentage of sub-G_1/G_0 cells (M1 peak) in DU-145 cells increased from 1.6% after 24 h to 21.0% after 72 h. The percentage of sub-G_1/G_0 cells in MDA-MB-231 cells increased from 2.1% after 24 h to 10.1% after 72 h (Fig. 3). In both cell lines, the amount of fragmented DNA is not significantly increased over control (DMSO) until after 72 h of treatment. Agarose gel electrophoresis of DNA isolated from EF24-treated MDA-MB-231 cells also shows a characteristic smear that is indicative of DNA fragmentation (data not shown). Thus, it appears that this arrest after 48 h precedes the DNA fragmentation seen after 72 h. After the cells arrest in G2/M, they subsequently enter the final stages of apoptosis.

Activation of apoptosis

To determine the mechanism of EF24-induced cell death, we measured a number of markers of apoptosis.

Depolarization of mitochondrial membrane potential

Both MDA-MB-231 and DU-145 cells were treated with 20 μM EF24 for 0, 12, 24 and 48 h before labeling with 1 μg/ml JC-1 (Fig. 4). Both cell lines lose the ability to sequester the JC-1 dye in the mitochondrial

Fig. 3

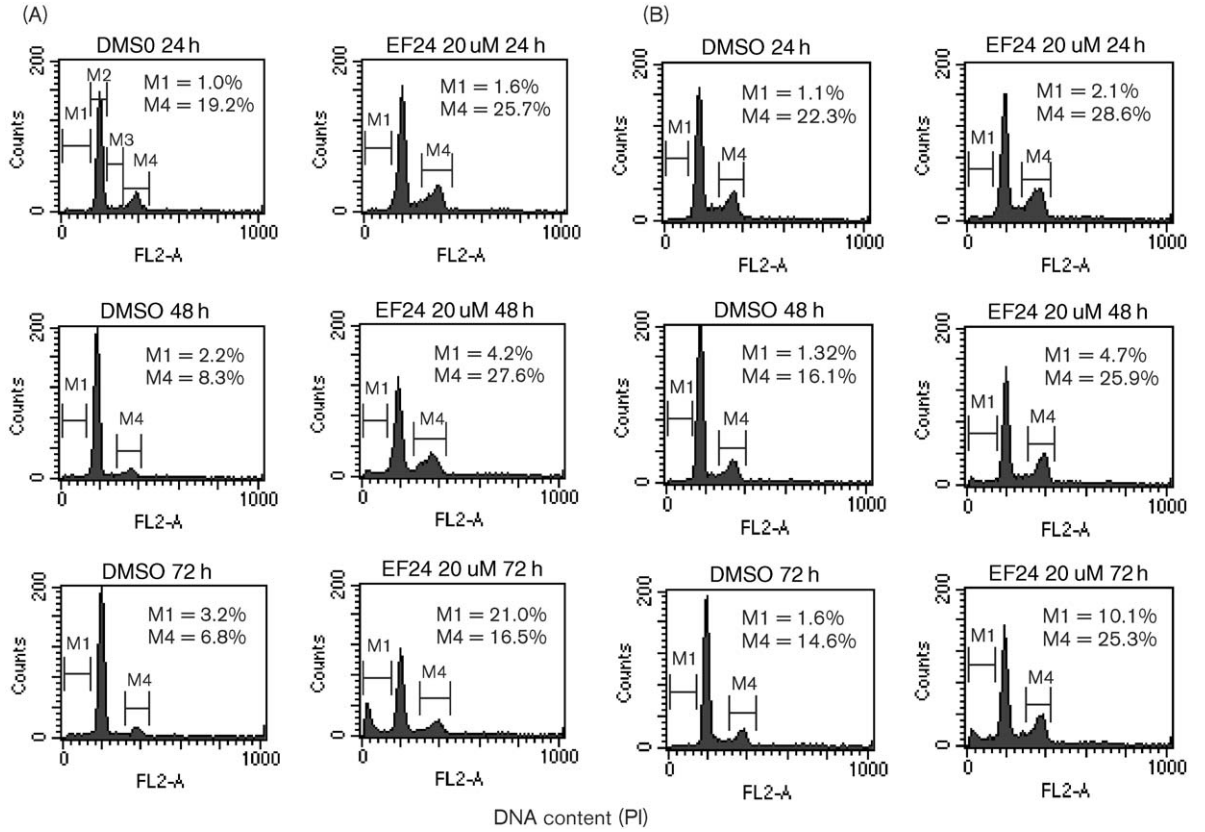

DNA content (PI) and cell cycle analysis of EF24-treated cells. DU-145 prostate cancer cells (A) and MDA-MB-231 breast cancer cells (B) were treated with EF24 for 24, 48 and 72 h. M1 = sub-G_1/G_0 peak, M2 = G_1 phase, M3 = S phase and M4 = G_2/M phase. Apoptosis was measured as percentage of cells containing hypodiploid amounts of DNA (sub-G_1/G_0 peak). EF24 seems to induce a G_2/M arrest after 48 h of treatment as shown by the increase in M4 over control. No substantial increase in M1 is seen until 72 h, indicating that the G_2/M arrest precedes DNA fragmentation. Graphs are representative of data collected from at least three experiments.

compartment following treatment with the compound, causing a time-dependent increase in green versus red fluorescence. To aid quantification, the dot-plots have been arbitrarily divided into quadrants. At 0 h, both breast and prostate tumor cells sequester more than 90% of the dye in the mitochondria, and show very little green fluorescence (6.0% for DU-145 cells, 4.4% for MDA-MB-231 cells). However, after 12 h with EF24, the green fluorescence increases significantly to 24.0% for the DU-145 cells and 24.3% for the MDA-MB-231 cells. Mitochondrial membrane potential continues to decrease by 24 h, and after 48 h, 50.0% of the DU-145 cells and 80.4% of the MDA-MB-231 cells are fluorescing green.

Activation of caspase-3

The EF24-induced activation of caspase-3 in DU-145 and MDA-MB-231 cells over a 72-h period is depicted in Figure 5. The assay uses a caspase-3 substrate that has been conjugated to two fluorophores that are normally quenched. Upon activation of caspase-3, the folded peptide is cleaved and the fluorophores provide a high intensity fluorescent signal at a visible wavelength. This is seen in the histogram plots as a right shift in the curve. To aid in the quantification, M1 has been arbitrarily set at the same FL2-H value for all the graphs, resulting in control caspase-3 activity of approximately 2–5%. Efficient activation of caspase-3 occurs after 24 h EF24 treatment in both cell lines, resulting in a fluorescence increase to 18.6% in the DU-145 cells and 38.6% in the MDA-MB-231 cells. Increasing fluorescence intensity is seen after 48 h, and by 72 h, 47.2% of the DU-145 cells and 82.6% of the MDA-MB-231 cells show active caspase-3.

Induction of PS externalization

Figure 6 shows the results of bivariate FITC–Annexin-V/PI flow cytometry analysis of DU-145 and MDA-MB-231 cells after treatment with EF24 for different times. The lower left quadrant (Quadrant III) of the cytograms shows the viable cells, which exclude PI and are negative for FITC–Annexin-V binding. The upper left quadrant (Quadrant I) represents necrotic cells, which show PI

Fig. 4

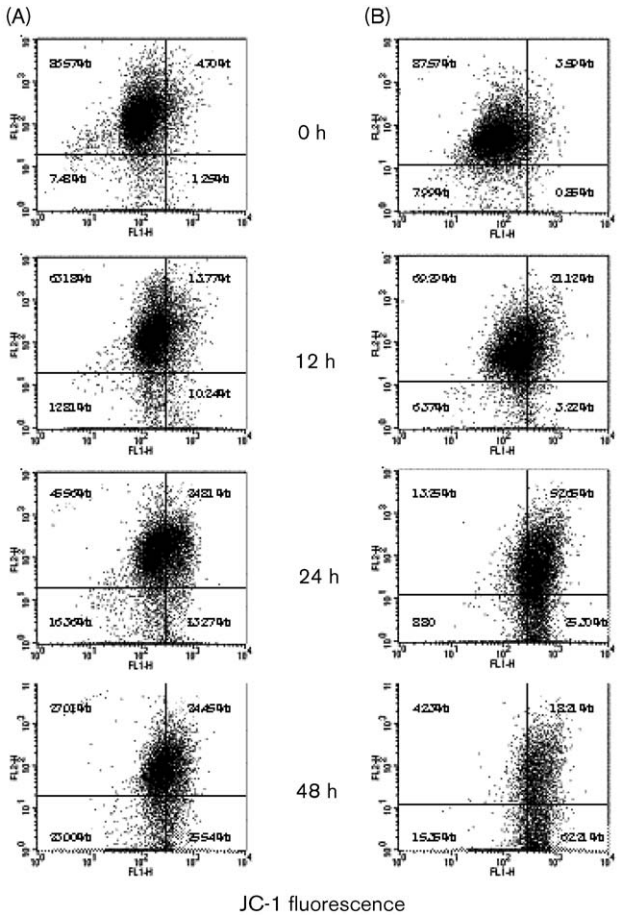

EF24-induced depolarization of mitochondrial membrane potential. DU-145 cells (A) and MDA-MB-231 cells (B) were treated with 20 μM EF24 for 0, 12, 24 and 48 h, and the relative intensity of green versus red fluorescence was plotted. The JC-1 dye emits a red fluorescence when sequestered in healthy mitochondria and cells with depolarized mitochondrial membrane potential show a green fluorescence. Each dot represents a single cell and the plots were divided arbitrarily into quadrants with the fluorescence intensities shown in each quadrant. Graphs are representative of data collected from at least three experiments.

uptake, but are negative for FITC–Annexin-V binding. The upper right quadrant (Quadrant II) represents the late apoptotic cells, which are positive for both PI and FITC–Annexin-V. The lower right quadrant (Quadrant IV) represents cells in the early stages of apoptosis. These cells demonstrate FITC–Annexin-V binding, but are negative for PI uptake, suggesting that there is no leaking of the plasma membrane (an intact cytoplasmic membrane). After EF24 treatment, the DU-145 cell population in early apoptosis (Annexin-V–FITC$^+$/PI$^-$, Quadrant IV) increased gradually from a control of 3.5% to 6.3% after 24 h, 14.4% after 48 h and 17.7% after 72 h. The percentage of DU-145 cells in late apoptosis (Annexin-V–FITC$^+$/PI$^+$, Quadrant II) increased from a control of 4.0% to 39.8% after 72 h. The percentage of MDA-MB-231 cells in early apoptosis increased from a control of 2.5% to 6.9% after 24 h, 19.0% after 48 h and 25.3% after 72 h. Similarly the cell population in late apoptosis increased from a control of 2.8% to 45.6% after 72 h. The pan-caspase inhibitor z-VAD-fmk has been demonstrated to completely block apoptosis. After a 72-h treatment with both EF24 and z-VAD-fmk, the cell population in Quadrant IV was reduced to 12% for the DU-145 cells and 6.8% for the MDA-MB-231 cells.

EF24-induced redox changes in cancer cells

Production of ROS

We studied the effects of EF24 on the production of ROS in DU-145 prostate and MDA-MB-231 breast cancer cells using the peroxide-sensitive fluorescent probe DCF-DA. EF24 at 20 μM produced a time-dependent increase in intracellular ROS after treatment for 12, 24 and 48 h in both cell lines. Generation of ROS by DU-145 and MAD-MB-231 cells at 48 h is 35 and 55%, respectively (Fig. 7).

Direct interaction of EF24 with GSH/Trx-1 and depleting intracellular GSH

To determine whether EF24 reacts with GSH or Trx-1, we have measured their direct interactions *in vitro*. The absorbance spectrum of EF24 in PBS shows peaks around 325 nm and its content in solution can be monitored in a spectrophotometer. Separate addition of both GSH and Trx-1 to EF24 resulted in a time-dependent decrease in the absorbance, indicating EF24 had reacted with the cysteines in both GSH and Trx-1 (Fig. 8A). To determine the effects of EF24 on the thiol/disulfide redox status in intact cells, we measured the intracellular GSH concentrations in HT29 human colon adenocarcinoma cells after treatment with EF24 at 20 μM concentration for 90 min. Cells were extracted with 10% perchloric acid/0.2 M boric acid. The acid soluble GSH was then measured by HPLC as described [15]. Results indicate that intracellular GSH content decreased significantly after EF24 treatment and the decrease in GSH was not associated with an increase in the GSSG contents (Fig. 8B). The GSH depletion was not affected by overexpression of Bcl-x_L.

Discussion

In this study we have attempted to determine whether the cytotoxic activity of EF24 is due to apoptosis by examining some of the most accepted signs of cell death. These indicators occur in sequence beginning with depolarization of the mitochondria membrane, through caspase-3 activation and externalization of PS, to the final DNA fragmentation (sub-G_1/G_0 accumulation of DNA). In addition, we have found that EF24 reduces intracellular GSH and Trx-1, and increases the concentration of ROS. This balance shift, together with a high mitochondrial Ca^{2+} overload and low ATP production, most likely triggers opening of the mitochondrial permeability transition pores allowing facile diffusion of

Fig. 5

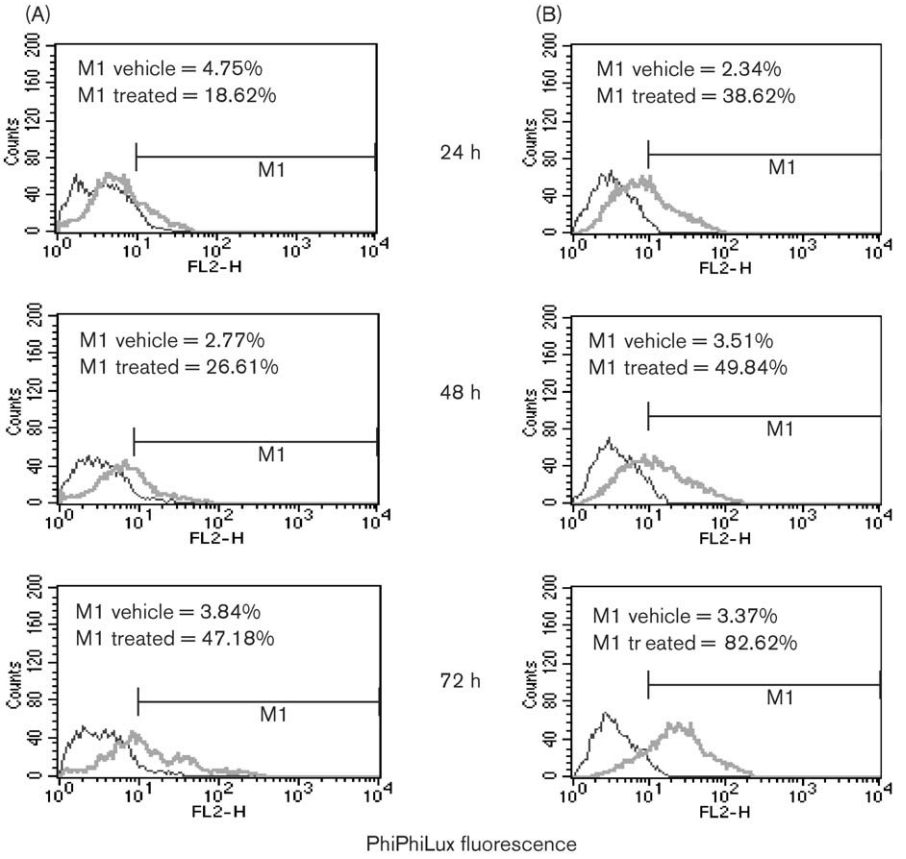

PhiPhiLux fluorescence and caspase-3 activation in EF24-treated cells. DU-145 cells (A) and MDA-MB-231 cells (B) were treated with 20 μM EF24 for 24, 48 and 72 h. Caspase-3 activation was measured by flow cytometry and detected as an increase in fluorescence intensity. Fluorescence results from the unquenching of two fluorophores following cleavage of the caspase-3 peptide substrate linking the fluorophores. The right-shifted curve represents cells treated with compound compared to the control curve. M1 = percentage of cells with active caspase-3. Graphs are representative of data collected from at least three experiments.

low-molecular-weight solutes across the inner membrane. The pore is composed of a complex of the voltage-dependent anion channel, the adenine nucleotide translocase and cyclophilin D at contact sites between the mitochondrial outer and inner membranes. Opening of the permeability transition pore not only activates the apoptotic pathway, but also stimulates necrotic cell death [16]. We will first discuss evidence that EF24 induces apoptosis in two human cancer cell lines and follow with what we believe to be the structural basis of the mechanism of action. In sum, the cytotoxic action of EF24 is most likely the consequence of multiple complex actions—partly from the apoptotic cascade and partly from other modes of cell death such as necrosis.

Inhibition of cell proliferation

To evaluate the effects of EF24 on cell cycle progression, we utilized a BrdU-incorporation assay [17] to measure the ability of EF24 to inhibit the proliferation of two highly malignant human cancer cell lines *in vitro*. Measurement of [^{3}H]thymidine incorporation into the DNA as cells enter the S phase has long been the traditional method for detection of cell proliferation. The thymidine analog, BrdU, is a well-established alternative to assays using [^{3}H]thymidine uptake [17]. When BrdU is incorporated into the DNA of actively proliferating cells followed by partial denaturation of double-stranded DNA, it can be detected immunochemically. This permits the quantitative assessment of cells actively synthesizing DNA.

EF24 at 10 μM inhibited cell proliferation by 70–80% in human prostate cancer cells (DU-145) and by 100% in human breast cancer cells (MDA-MB-231) at 24 and 48 h based on BrdU assays. The assays were performed by plating 20 000 cells/well on 96-well plates. However, assays for testing apoptosis were carried out by plating 1×10^6 cells on six-well plates because 10 000 cells are required for flow cytometry analysis. In this system, EF24 at 20 μM did not inhibit cell proliferation to the same

Fig. 6

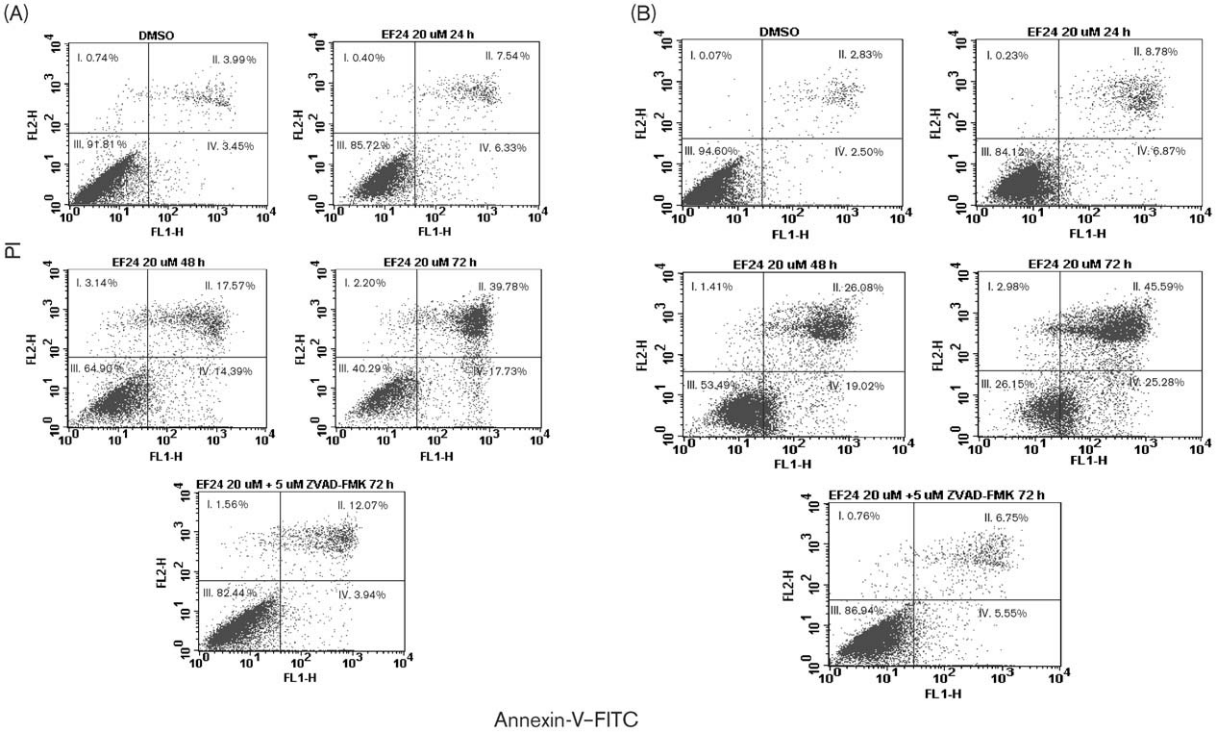

Annexin-V–FITC and EF24-induced PS exposure. DU-145 prostate cancer cells (A) and MDA-MB-231 breast cancer cells (B) were treated with 20 μM EF24 for 24, 48 and 72 h. Cells were stained with Annexin-V and PI to identify early and late apoptosis. Quadrant I: necrotic cells, Quadrant II: late apoptosis/necrosis, Quadrant III: viable cells and Quadrant IV: early apoptosis. Since Quadrant II contains both late apoptotic and necrotic cells, the percentage of necrotic cells in this quadrant after 72 h was measured by adding 5 μM z-VAD-fmk, a pan-caspase inhibitor that completely blocks apoptosis. Graphs are representative of data collected from at least three experiments.

extent as seen in the BrdU assays. This is demonstrated in Quadrant III for each of the dot plots shown in Fig. 6, which represents the number of viable cells (Annexin-V^-/PI^-) that remain following treatment with EF24 for 24, 48 and 72 h. One reason for the discrepancy between the BrdU incorporation assay and the apoptosis measurements may result from the light sensitivity of EF24. The compound degrades to 10% of the original activity in 10 h while it is kept on the laboratory bench at ambient temperature under fluorescent lights in a clear vial. Thus, 20 μM EF24 compromised by photodegradation was chosen for the apoptosis measurements. We expect that repetition in the dark would show a concentration dependence comparable to the BrdU experiments. Another reason for the discrepancy may be due to the differences in how each of the assays was conducted (i.e. different cell numbers and plate surface areas). Different overall cell concentrations in the two assay methods may well affect drug potency with regard to IC_{50} values.

Sub-G_1/G_0 accumulation of DNA

We first demonstrated that EF24 induced sub-G_1/G_0 accumulation of DNA in both human prostate (DU-145) and breast cancer (MDA-MB-231) cell lines by observing an increase in the sub-G_1/G_0 peak at 72 h compared with that at 24 h of EF24 treatment (M1 peak in Fig. 3). Sub-G_1/G_0 DNA accumulation was preceded by G_2/M arrest as evidenced by an increase in the M4 peak at 48 h of EF24 treatment as compared with that of DMSO control (Fig. 3). It should be noted that cells arrest their cell cycles in order to repair DNA damage. If the damage is repaired, the cells resume a normal cell cycle. If not, they take the apoptotic pathway. The mean percentage of G_2/M arrest was 30–35% at 48 h, while that of sub-G_1/G_0 DNA accumulation was approximately 7.5% at 72 h in both cell lines (data not shown). At 20 μM, EF24 apparently does not induce apoptosis in all the cells, since 63.5% of DU-145 and 64.6% of MDA-MB-231 cells are in G_1 and S phases, respectively, at 72 h (Fig. 3). At the same time, 40–50% of the cells are still viable by 72 h as shown in Quadrant III of Figure 6. EF24 may induce apoptosis as well as other modes of cell killing in both cell lines, although there are very few cells in Quadrant I that represent necrotic cells. The activity of curcumin on induction of sub-G_1/G_0 accumulation is approximately 1/4 to 1/2 that of EF24 in both cell lines (data not shown). This corresponds to a 2- to 10-fold increase in cytotoxic activity for EF24 over curcumin [4].

Fig. 7

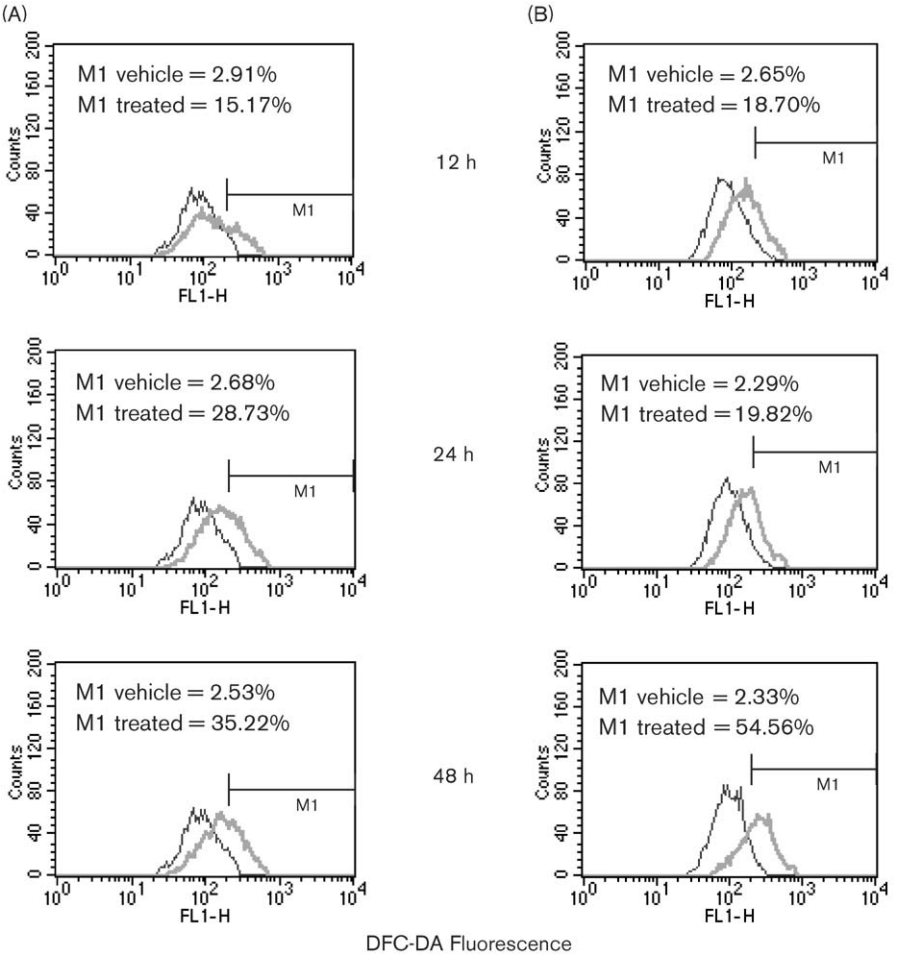

DCD-DA fluorescence and generation of ROS after treatment with EF24. DU-145 prostate cancer cells (A) and MDA-MB-231 breast cancer cells (B) were treated with 20 μM EF24 for 8, 24 and 48 h. The right-shifted curve represents cells treated with compound compared to the control curve. M1 = percentage of cells with activated ROS species. Graphs are representative of data collected from at least three experiments.

Depolarization of the mitochondrial membrane potential

Mitochondrial membrane depolarization is an early sign of apoptosis. Upon induction of apoptosis, mitochondria lose the ability to sequester charged cations [6]. Cytochrome *c* from the mitochondrial intermembrane space is released into the cytosol following the depolarization [6,18]. In the cytosol, cytochrome *c* binds to apoptosis-inducing factor (apaf-1) and pro-caspase-9 in the presence of dATP to form apoptosome [19]. This complex activates caspase-9, which in turn activates caspase-3 [20]. Curcumin has been demonstrated to induce mitochondrial depolarization [21,22], release cytochrome *c* and activate caspase-3 [23]. EF24's depolarizing action in both cancer cell lines was monitored as a time-dependent increase in cells with green fluorescence (from JC-1 dye in the cytosol) as compared with red fluorescence (from JC-1 dye in the mitochondria) during the 48 h following drug treatment. Human breast cancer cells (MDA-MB-231) depolarized the mitochondrial membrane in 80% of the cells, while human prostate cancer cells (DU-145) exhibited the same phenomenon in only 50% of the cells at 48 h. The former cell line appears to be more sensitive to EF24 since inhibition of cell proliferation was 100%, while that for DU-145 cells was 70–80% at 10 μM for 24–48 h (Fig. 2).

Caspase-3 activation

Activation of caspases, a family of cysteine proteases in many multicellular organisms [16], is an essential step in various forms of apoptosis [24]. The enzymes' role in programmed cell death is highly conserved. Caspase-3 is one of these agents most frequently activated during the process of apoptosis. In response to pro-apoptotic stimuli, the 32-kDa pro-caspase-3 is processed to an active enzyme consisting of two subunits of 17 and 12 kDa.

Fig. 8

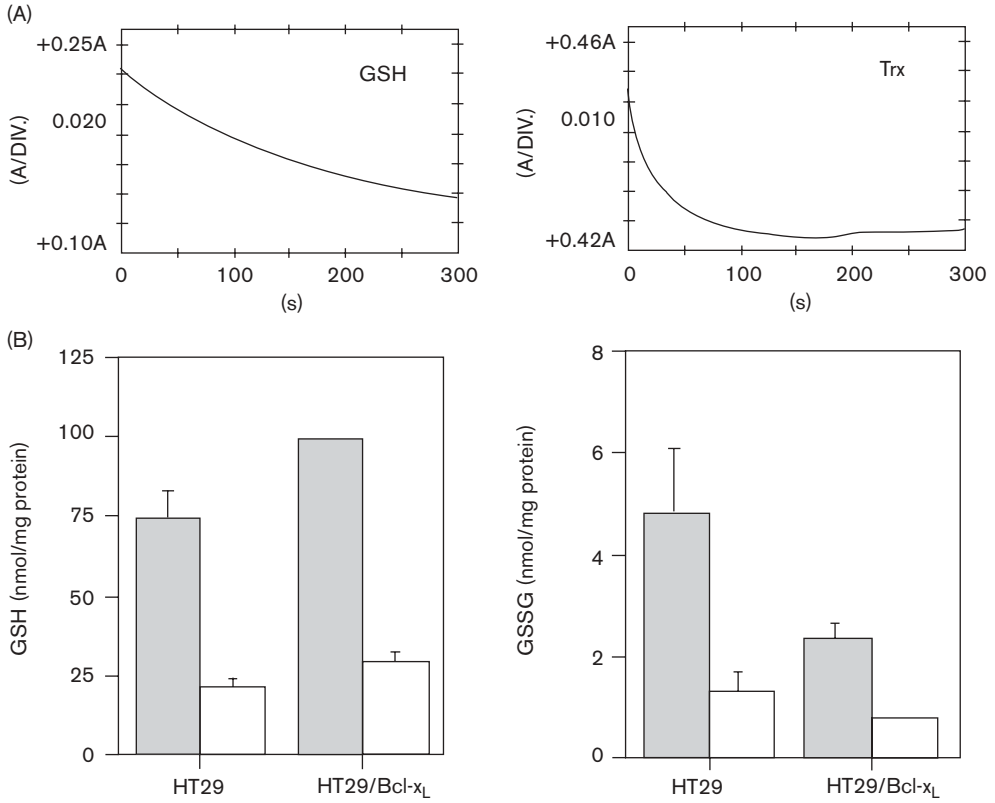

(A) Interaction of EF24 for reactions with GSH and Trx-1. EF24 was added to 20 μM (or indicated concentration) into 1 ml of PBS (pH 7.0) solution in disposable cuvettes. The reaction was monitored at 325 nm for 10 min at 30°C. A decrease in absorbance indicates EF24 has reacted with GSH/Trx-1 and changed its spectroscopic character. (B) Depletion of GSH in HT29 cells treated with EF24. HT29 control and Bcl-x_L overexpressing cells were treated with 20 μM EF24 for 90 min. Intracellular GSH and GSSG were measured by HPLC. Cells undergoing apoptosis export GSH as a consequence of caspase activation. However, EF24-induced GSH depletion was not inhibited by overexpression of Bcl-x_L, indicating the reaction between EF24 and GSH occurs early during cell death, and is likely to be upstream of caspase activation. Gray bars = control; white bars = treatment.

Activated caspase-3 is essential for the progression of apoptosis, resulting in the degradation of cellular proteins, apoptotic chromatin condensation and DNA fragmentation [25].

In our experiments, EF24-induced caspase-3 activation in a time-dependent manner up to 72 h was manifested by an increase in PhiPhiLux fluorescence on the FL_2H axis (*x*-axis) in both cell lines (Fig. 5). However, caspase activation in MDA-MB-231 cells is almost 2 times greater than that in DU-145 cells. Again, this suggests that the MDA-MB-231 cells are more sensitive to EF24 than the DU-145 cells (Fig. 2). It is noteworthy that curcumin at 25 μM has been reported to induce the activation of caspase-3 in HL60 leukemic cells [23].

Externalization of PS

In the early stages of apoptosis, PS translocates from the inner side of the plasma membrane to the outer layer, thus exposing PS at the external surface of the cell. Studies have demonstrated that the exposure is due partially to the activation of the caspase cascade [26]. Annexin-V, a calcium-dependent phospholipid-binding protein, has a high affinity for PS and can be used as a sensitive probe to measure the exposure of this phospholipid on the cell membrane [13]. During the initial stages of apoptosis, the cell membrane remains intact. However, during later stages, the cell membrane loses its integrity and becomes leaky. Therefore, the measurement of Annexin-V binding to the cell surface can be performed in conjunction with a dye-exclusion test to establish the integrity of the cell membrane and determine the stage of apoptosis. A common dye for this application is PI, which induces a red fluorescence of the DNA in cells with a damaged membrane, but is excluded in cells with an intact membrane. Hence, during the initial phase of apoptosis, the cells are still able to exclude PI and therefore do not show any red fluorescence signal similar to that of living cells.

The EF24- induced externalization of PS at the plasma membrane was demonstrated by a time-dependent increase in the majority of cells accumulated in Quadrant II (late apoptosis) during 72 h of treatment in both breast and prostate cell lines. Early and late apoptotic cells (quadrants IV + II) in the two cell lines are 80 and 60%, respectively, again reflecting more EF24 sensitivity for the former cells (Fig. 2). The pan-caspase inhibitor z-VAD-fmk inhibits PS exposure in both cell lines (Fig. 6), suggesting that blockade of PS translocation is caused by the caspase activation.

ROS

ROS are generated intracellularly by means of a variety of processes, e.g. as byproducts of normal aerobic metabolism or as second messengers in various signal transduction pathways [27]. ROS have been implicated in the regulation of diverse cellular functions including defense against pathogens, intracellular signaling, transcriptional activation, proliferation and apoptosis. Intercellular levels of ROS are influenced by a number of endogenous and exogenous processes, and controlled by several radical scavenging enzymes. Exogenous agents that induce ROS formation include anticancer agents, UV light and various cytokines. At the cellular level, oxidant injury elicits a wide spectrum of responses ranging from proliferation to growth arrest to cell death [28]. Researchers have demonstrated that ROS production may play a role in curcumin-induced apoptosis [29,30].

The redox state of the cell is primarily a consequence of the precise balance between the levels of ROS and endogenous thiol buffers present in the cell, such as GSH and Trx-1. The latter entities protect cells from oxidative damage and modulate apoptotic signals [31]. Cytotoxic and chemotherapeutic agents reduce the intracellular levels of GSH not only by elevating ROS, but also by extruding GSH from the cells [32]. The details as to how depletion of cellular GSH, Trx-1 and thiol proteins induces apoptosis are still obscure. It has been demonstrated that depletion of cellular GSH induces the initial phase of ROS generation at low levels [33]. The ROS in turn open the mitochondrial pore, leading to mitochondrial depolarization [16], which leads to the second phase of an explosive burst of ROS production at much higher levels. The source of this burst is the mitochondrial electron transport chain [33]. In the present work, EF24 induces a relatively high level of ROS after 48 h of treatment in both cell lines, which coincides nicely with the data from Figures 3–6. The observations imply that the major apoptotic activity in these cell lines occurs between 24 and 48 h. Throughout all our experiments a common thread is that the MDA-MB-231 cells are more sensitive to EF24 than DU-145 cells. However, this does not necessarily mean that breast cancer cells are generally more sensitive to EF24 than prostate cancer cells, based on the results tested against a panel of 60 human cancer cell lines by the National Cancer Institute [4].

Direct interaction of EF24 with GSH and Trx-1

In parallel with our studies on drug-induced apoptosis, we have examined a mechanism of action for EF24 that is directly related to the structure of the drug. The cellular thiol/disulfide pool plays a critical role in controlling oxidative stress and redox-dependent signal transductions. GSH and Trx-1 are two of the most abundant molecules with reactive sulfhydryl groups.

Curcumin, an α,β-unsaturated ketone, is a classic Michael acceptor [34,35] which forms an irreversible covalent adduct with the sulfhydryl (SH) group of multiple target molecules such as GSH [36–39]. Trx-1 is a M_r 12 000 protein incorporating a redox-active pair of cysteine residues. The compound is important as a disulfide reducing agent and is crucial for processes such as ribonucleotide reduction and transcription factor modulation [40]. GSH and reduced Trx-1 levels are closely tied to apoptosis. It has been suggested that inactivation of Trx reductase by unsaturated Mannich bases may be one of the causes of apoptotic death in human tumor cells [41–47]. A putative mechanism for irreversible inactivation of Trx reductase by α,β-unsaturated Mannich bases that possess one or two electrophilic centers and react with thiols has been described [48]. EF24, an α,β-unsaturated ketone, is likewise a strong Michael acceptor [4] as shown by its reactions with GSH and Trx-1 (Fig. 8A). In this respect, it most certainly behaves in a manner similar to the less-electrophilic curcumin molecule. EF24 not only increases production of ROS (Fig. 7), but also reduces intracellular GSH and GSSG in wild-type and even in Bcl-x_L overexpressed human colon cancer cells (Fig. 8B). Thus, even Bcl-x_L is unable to prevent the action of EF24, although Bcl-x_L possesses anti-apoptotic properties that are attributed to its ability to prevent translocation of cytochrome *c* to the cytosol and thereby interfere with the subsequent depolarization of the mitochondrial membrane [49], activation of cytosolic caspases and apoptosis [6,50,51]. Thus, as we have demonstrated above (Figs 3–6), the oxidative stress caused by EF24 contributes to the depolarization of the mitochondrial membrane potential and the subsequent downstream events, such as caspase activation and substrate cleavage [31,52].

In summary, the principle biological roles of EF24 may well depend on its action as a Michael acceptor. We have demonstrated that F (fluoride) at the *ortho* position, but not *meta* or *para* positions, of the terminal aromatic rings confers the most potent anticancer activity [4]. It is of interest that unsubstituted OH (hydroxyl) groups at the *ortho* position, but not *meta* or *para* positions, of the terminal aromatic rings of a substituted cyclopentanone

proved to exhibit the best induction of quinone reductase, enhancing the nucleophilic reactivity of the SH groups. However, the exact mechanism is unknown, since potency increases stimulated by inducers of quinone reductase bearing *ortho*-hydroxy groups could not be ascribed to increased electrophilicity of the β-vinyl carbon atoms of the Michael acceptor [53]. The same group recently demonstrated that all inducers react covalently with thiols at rates that are closely related to their potencies [37].

Summary, conclusions and prospects

The structurally simple and symmetric curcumin analog EF24 induces cell cycle arrest and apoptosis in human breast cancer (MDA-MB-231) and human prostate cancer (DU-145) cells as substantiated by ROS production, caspase-3 activation, PS externalization and DNA fragmentation. The compound likewise promotes depolarization of the mitochondrial membrane potential, suggesting that disruption of mitochondrial function is one possible origin of apoptosis. This interpretation is strengthened by the observation that EF24 reduces intracellular GSH and its oxidized form, GSSG, in wild-type and Bcl-x_L overexpressing HT29 cancer cells. Further evidence derives from the reaction between Michael acceptor EF24 and the thiol-containing substrates GSH and Trx-1. These observations suggest that EF24, at least with respect to proteins and mediators bearing the SH group, has the potential to modulate the action of multiple targets. Accordingly, the specific action of EF24 in different cells may depend on the concentration and accessibility of the compound to molecules bearing the SH group [53]. The existence of multiple targets may prove to be a decisive advantage, since it can reduce the occurrence of cells resistant to EF24, while diminishing toxicity. The apparent low toxicity of EF24 [4] can be understood from this viewpoint.

References

1 Aggarwal BB, Kumar A, Bharti AC. Anticancer potential of curcumin: preclinical and clinical studies. *Anticancer Res* 2003; **23**:363–398.
2 Satoskar RR, Shah SJ, Shenoy SG. Evaluation of anti-inflammatory property of curcumin (diferuloylmethane) in patients with post-operative inflammation. *Int J Clin Pharmacol Ther Toxicol* 1986; **24**:651–654.
3 Shoba G, Joy D, Joseph T, Majeed M, Rajendran R, Srivinas PS. Influence of piperine on the in animals pharmacokinetics of curcumin and human volunteers. *Planta Med* 1998; **64**:353–356.
4 Adams BK, Ferstl EM, Davis MC, Herold M, Kurtkaya S, *et al.* Synthesis and biological evaluation of novel curcumin analogs as anticancer and anti-angiogenesis agents. *Bioorg Med Chem* 2004; **12**:3871–3883.
5 Slater A, Stefan C, Nobel I, Van Den Dobbelsteen DJ, Orrenius S. Intracellular redox changes during apoptosis. *Cell Death Different* 1996; **3**:57–62.
6 Kluck RM, Bossy-Wetzel E, Green DR, Newmeyer JA. The release of cytochrome C from mitochondria: a primary site for *bcl-2* regulation of apoptosis. *Science* 1997; **275**:1132–1136.
7 Eischen CM, Kottke TJ, Martins LM, Basi GS, Tung JS, Earnshaw WC, *et al.* Comparison of apoptosis in wild-type and Fas-resistant cells: chemotherapy-induced apoptosis is not dependent on Fas/Fas ligand interactions. *Blood* 1997; **90**:935–943.
8 Cai J, Chen Y, Murphy TJ, Jones DP, Sartorelli AC. Role of caspase activation in butyrate-induced terminal differentiation of HT29 colon carcinoma cells. *Arch Biochem Biophys* 2004; **424**:119–127.
9 Hardonk MJ, Harms G. The use of 5′-bromodeoxyuridine in the study of cell proliferation. *Acta Histochem Suppl* 1990; **39**:99–108.
10 Armstrong JS, Hornung B, Lecane P, Jones DP, Knox SJ. Rotenone-induced G_2/M cell cycle arrest and apoptosis in a human B lymphoma cell line PW. *Biochem Biophys Res Commun* 2001; **289**:973–978.
11 Kluza J, Lansiaux A, Wattez N, Hildebrand M-P, Leonce S, Pierre A, *et al.* Induction of apoptosis in HL-60 leukemia and B16 melanoma cells by the acronycine derivative S23906-1. *Biochem Pharmacol* 2002; **63**:1443–1452.
12 Salvioli S, Ardizzoni A, Franceschi C, Cossarizza A. JC-1, but not $DiOC_6(3)$ or rhodamine 123, is a reliable fluorescent probe to assess DY changes in intact cells: implications for studies on mitochondrial functionality during apoptosis. *FEBS Lett* 1997; **411**:77–82.
13 Hirata H, Takahashi A, Kobayashi S, Yonehara S, Sawai H, Okazaki T, *et al.* Caspases are activated in a branched protease cascade and control distinct downstream processes in fas-induced apoptosis. *J Exp Med* 1998; **187**:587–600.
14 Vermes I, Haanen C, Steffens-Nakken H, Reutelingperger C. A novel assay for apoptosis—flow cytometric detection of phosphatidylserine expression on early apoptotic cells using fluorescein labeled Annexin-V. *J Immunol Methods* 1995; **184**:39–51.
15 Jones DP. Redox state of GSH/GSSG couple: assay and biological significance. *Methods Enzymol* 2002; **348**:93–112.
16 Crompton M. The mitochondrial permeability transition pore and its role in cell death. *Biochem J* 1999; **341**:233–249.
17 Ternynck T, Portsmann T, Avrameas S. Enzyme immunoassay using a monoclonal antibody against 5-bromo-2-deoxyuridine for the assessment of lymphoid cell proliferation. *Methods Enzymol* 1987; **150**:117–129.
18 Kuwana T, Newmeyer DD. Bcl-2-family proteins and the role of mitochondria in apoptosis. *Curr Opin Cell Biol* 2003; **15**:691–699.
19 Zou H, Henzel WJ, Liu X, Lutschg A, Wang X. Apaf-1, a human protein homologous to *C. elegans* CED-4, participates in cytochrome *c*-dependent activation of caspase-3. *Cell* 1997; **90**:405–413.
20 Li P, Nijhawan D, Budihardjo I, Srinivasula SM, Ahmad M, Alnemri ES, *et al.* Cytochrome *c* and dATP-dependent formation of Apaf-1/caspase-9 complex initiates an apoptotic protease cascade. *Cell* 1997; **91**:479–89.
21 Pan MH, Chang WL, Lin-Shiau SY, Ho CT, Lin JK. Induction of apoptosis by garcinol and curcumin through cytochrome *c* release and activation of caspases in human leukemia HL-60 cells. *J Agric Food Chem* 2001; **49**:1464–1474.
22 Morin D, Barthelemy S, Zini R, Labidalle S, Tillement JP. Curcumin induces the mitochondrial permeability transition pore mediated by membrane protein thiol oxidation. *FEBS Lett* 2001; **495**:131–136.
23 Anto RJ, Mukhopadhyay A, Denning K, Aggarwal BB. Curcumin (diferuloylmethane) induces apoptosis through activation of caspase-8, BID cleavage and cytochrome *c* release: its suppression by ectopic expression of Bcl-2 and Bcl-x_L. *Carcinogenesis* 2002; **23**:143–150.
24 Nicholson DW, Thornberry NA. Caspases: killer proteases. *Trends Biochem Sci* 1997; **22**:297–306.
25 Thornberry NA, Lazebnik Y. Caspases: enemies within. *Science* 1998; **281**:1312–1316.
26 Huigsloot M, Tijdens IB, Mulder GJ, Van de Water B. Differential regulation of phosphatidylserine externalization and DNA fragmentation by caspases in anticancer drug-induced apoptosis of rat mammary adenocarcinoma MTLn3 cells. *Biochem Pharmacol* 2001; **62**:1087–1097.
27 Gamaley IA, Klyubin IV. Roles of reactive oxygen species: signaling and regulation of cellular function. *Rev Cytol* 1999; **188**:203–238.
28 Martindale JL, Holbrook NJ. Cellular response to oxidative stress: signaling for suicide and survival. *J Cell Physiol* 2002; **192**:1–15.
29 Bhaumik S, Anjum R, Rangaraj N, Pardhasaradhi BVV, Khar A. Curcumin mediated apoptosis in AK-5 tumor cells involves the production of reactive oxygen intermediates. *FEBS Lett* 1999; **456**:311–314.
30 Khar A, Mubarak A, Pardhasaradhi BVV, Begum Z, Anjum R. Antitumor activity of curcumin is mediated through the induction of apoptosis in AK-5 tumor cells. *FEBS Lett* 1999; **445**:165–168.
31 Davis W. Jr, Ronai Z, Tew KD. Cellular thiols and reactive oxygen species in drug-induced apoptosis. *J Pharmacol Exp Ther* 2001; **296**:1–6.
32 Ghibelli L, Coppola S, Rotilio G, Lafavia E, Maresca V, Ciriolo MR. Non-oxidative loss of glutathione in apoptosis via GSH extrusion. *Biochem Biophys Res Commun* 1995; **216**:313–320.
33 Tan S, Sagara Y, Liu Y, Maher P, Schubert D. The regulation of reactive oxygen species production during programmed cell death. *J Cell Biol.* 1998; **141**:1423–1432.
34 Dinkova-Kostova AT, Talalay P. Relation of structure of curcumin analogs to their potencies as inducers of Phase 2. *Carcinogenesis* 1999; **20**:911–914.

35 Dragovich PS, Prins TJ, Zhou R, Johnson TO, Hua Y, Luu HT, *et al.* Structure-based design, synthesis, and biological evaluation of irreversible human rhinovirus 3C protease inhibitors. 8. Pharmacological optimization of orally bioavailable 2-pyridone-containing peptidomimetics. *J Med Chem* 2003; **46**:4572–4585.
36 Awasthi S, Pandya U, Singhal SS, Lin JT, Thiviyanathan V, Seifert Jr WE, *et al.* Curcumin–glutathione interactions and the role of human glutathione S-transferase P1-1. *Chem-Biol Interact* 2000; **128**:19–38.
37 Dinkova-Kostova AT, Holtzclaw WD, Cole RN, Itoh K, Wakabayashi N, Katoh Y, *et al.* Direct evidence that sulfhydryl groups of Keap1 are the sensors regulating induction of phase 2 enzymes that protect against carcinogens and oxidants. *Proc Natl Acad Sci USA* 2002; **99**:11908–11913.
38 Schaefer WH, Harris TM, Guengerich FP. Reaction of the model thiol 2-mercaptoethanol and glutathione with methylvinylmaleimide, a Michael acceptor with extended conjugation. *Arch Biochem Biophys* 1987; **257**:186–193.
39 Sausen PJ, Elfarra AA. Reactivity of cysteine S-conjugate sulfoxides: formation of S-[1-chloro-2-(*S*-glutathionyl)vinyl]-L-cysteine sulfoxide by the reaction of *S*-(1,2-dichlorovinyl)-L-cysteine sulfoxide with glutathione. *Chem Res Toxicol* 1991; **4**:655–660.
40 Arner ES, Holmgren A. Physiological functions of thioredoxin and thioredoxin reductase. *Eur J Biochem* 2000; **267**:6102–6109.
41 Baker A, Payne CM, Briehl MM, Powis G. Thioredoxin, a gene found overexpressed in human cancer, inhibits apoptosis *in vitro* and *in vivo*. *Cancer Res* 1997; **57**:5162–5167.
42 Nicole A, Santiard-Baron D, Ceballos-Picot I. Direct evidence for glutathione as mediator of apoptosis in neuronal cells. *Biomed Pharmacother* 1998; **52**:349–355.
43 Si F, Ross GM, Shin SH. Glutathione protects PC12 cells from ascorbate- and dopamine-induced apoptosis. *Exp Brain Res* 1998; **23**:263–268.
44 Powis G, Kirkpatrick DL, Angulo M, Baker A. Thioredoxin redox control of cell growth and death and the effects of inhibitors. *Chemo-Biol Interact* 1998; **111/112**:23–34.
45 Anderson CP, Tsai JM, Meek WE, Liu RM, Tang Y, Forman HJ, *et al.* Depletion of glutathione by buthionine sulfoxine is cytotoxic for human neuroblastoma cell lines via apoptosis. *Exp Cell Res* 1999; **246**:183–192.
46 Higuchi Y, Matsukawa S. Glutathione depletion induces giant DNA and high-molecular-weight DNA fragmentation associated with apoptosis through lipid peroxidation and protein kinase C activation in C6 glioma cells. *Arch Biochem Biophys* 1999; **363**:33–42.
47 Powis G, Montfort WR. Properties and biological activities of thioredoxins. *Annu Rev Biophys Biomol Struct* 2001; **30**:421–455.
48 Davioud-charvet E, McLeish MJ, Veine DM, Giegel D, Arscott LD, Andricopulo AD, *et al.* Mechanism-based inactivation of thioredoxin reductase from *Plasmodium falciparum* by Mannich bases. Implication for cytotoxicity. *Biochemistry* 2003; **42**: 13319–13330.
49 Dairaku N, Kato K, Honda K, Koike T, Iijima K, Imatani A, *et al.* Oligomycin and antimycin A prevent nitric oxide-induced apoptosis by blocking cytochrome c leakage. *J Lab Clin Med* 2004; **143**: 143–151.
50 Kim CN, Wang X, Huang Y, Ibrado AM, Liu L, Fang G, *et al.* Overexpression of Bcl-x_L inhibits ara-C-induced mitochondrial loss of cytochrome *c* and other perturbations that activate the molecular cascade of apoptosis. *Cancer Res* 1997; **57**:3115–3120.
51 Yang J, Liu X, Bhalla K, Kim CN, Ibrado AM, Cai J, *et al.* Prevention of apoptosis by Bcl-2:release of cytochrome *c* from mitochondria blocked. *Science* 1997; **275**:1129–1132.
52 Jeng JH, Wang YJ, Chang WH, Wu HL, Li CH, Uang BJ, *et al.* Reactive oxygen species are crucial for hydroxychavicol toxicity toward KB epithelial cells. *Cell Mol Life Sci* 2004; **61**:83–96.
53 Dinkova-Kostova AT, Masshia MA, Bozak RE, Hicks RJ, Talalay P. Potency of Michael reaction acceptors as inducers of enzymes that protect against carcinogenesis depends on their reactivity with sulfhydryl groups. *Proc Natl Acad Sci USA* 2001; **98**:3404–3409.